First principles investigation of defect energy levels at semiconductor-oxide interfaces: Oxygen vacancies and hydrogen interstitials in the $Si-SiO_2-HfO_2$ stack

Peter Broqvist,[a] Audrius Alkauskas, Julien Godet,[b] and Alfredo Pasquarello
Institute of Theoretical Physics, Ecole Polytechnique Fédérale de Lausanne (EPFL), CH-1015 Lausanne, Switzerland and Institut Romand de Recherche Numérique en Physique des Matériaux (IRRMA), CH-1015 Lausanne, Switzerland

(Received 8 August 2008; accepted 24 September 2008; published online 16 March 2009)

We introduce a scheme for the calculation of band offsets and defect energy levels at semiconductor-oxide interfaces. Our scheme is based on the use of realistic atomistic models of the interface structure and of hybrid functionals for the evaluation of the electronic structure. This scheme is herein applied to the technologically relevant $Si-SiO_2-HfO_2$ stack. Calculated band offsets show a very good agreement with experimental values. In particular, we focus on the energy levels of the oxygen vacancy defect and the interstitial hydrogen impurity. The defect levels are aligned with respect to the interface band structure and determined for varying location in the dielectric stack. The most stable charge states are identified as the Fermi level sweeps through the silicon band gap. © *2009 American Institute of Physics*. [DOI: 10.1063/1.3055347]

I. INTRODUCTION

The replacement of SiO_2 with an oxide of higher dielectric constant (high-κ) (Ref. 1) has dramatically brought to the forefront our need for developing a more extended understanding of the atomic and electronic properties of typical defects in the new oxides. First principles modeling approaches are expected to provide a description of the atomic configurations of the unknown defects together with a characterization of their electronic energy levels with respect to the relevant band edges. However, the achievement of this target still faces several difficulties.[2]

Two aspects need particular attention. The first concerns the modeling of the interfacial transition region, which is generally characterized by a nontrivial connection between the crystalline semiconductor and the disordered oxide. To achieve a reliable band alignment at the interface, it is critical to provide a realistic description of the atomistic structure in this region.[3–5] Indeed, previous density functional studies on crystalline-crystalline interfaces have revealed a strong sensitivity of the band offsets on the adopted model of the interfacial bonding pattern.[3,4] Therefore, it is important to ensure that the transition region is smooth in terms of bond parameters and coordination.[5–9] For the $Si-SiO_2$ interface, such a choice led to variations of 0.1–0.2 eV in the calculated band offsets.[10,11] Furthermore, it is important to describe the amorphous nature of the oxide in order to capture the specific properties of interfacial defects.[5,12–14]

The second aspect concerns the method for describing the electronic structure. Density functional calculations of band offsets describe the electronic and atomic arrangements at the interface in a self-consistent way.[15–19] However, the most common approximations to the exchange-correlation energy, i.e., the generalized-gradient approximation and the local density approximation, lead to significant underestimations of band gaps, thereby impairing the reliability of calculated band offsets and defect levels. Previous theoretical work shows that band-offset errors for semiconductor-oxide interfaces can reach several eV.[3,8,9,20] Moreover, this discrepancy directly affects the determination of defect levels, making comparisons with experiment ambiguous. Therefore, it is ineluctable to address the band-gap problem going beyond semilocal approximations to density functional theory. Many-body perturbation theory in the *GW* approximation is the method of choice for calculating band offsets[21,22] and defect levels[23,24] but remains computationally demanding and therefore limited to small-sized systems. For instance, the study of realistic semiconductor-oxide interfaces in which the oxide is noncrystalline[5,8,9] is severely hindered.

In this work, we address band offsets and defect levels at semiconductor-oxide interfaces through the use of reliable interface models and hybrid functionals. These functionals incorporate a fraction of Hartree–Fock exchange, leading to a higher accuracy[25] and improved band gaps[26,27] compared to semilocal functionals. We focus on the technologically relevant $Si-SiO_2-HfO_2$ stack. First, we model the interface structure accounting for the occurrence of a SiO_2 interlayer and for the amorphous nature of the near-interface oxide and determine the band alignment at the interface. Then, we consider two kinds of oxide defects, the oxygen vacancy and the interstitial hydrogen, and align their energy levels to the interface band structure. For these defects, we calculate the formation energies for varying location across the dielectric stack and determine the stable charge states as the Fermi level sweeps through the silicon band gap.

II. METHODS

In the present work, the structural models were generated and structurally relaxed through the use of the semilocal

[a]Electronic mail: peter.broqvist@epfl.ch.
[b]Present address: PhyMat, University of Poitiers - CMRS, SP2MI - BP 30179, 86962 Futuroscope, France.

Downloaded 31 Mar 2009 to 128.178.157.61. Redistribution subject to AIP license or copyright; see http://jap.aip.org/jap/copyright.jsp

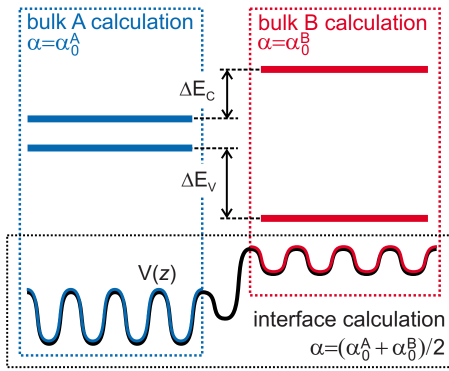

FIG. 1. (Color online) Schematic presenting the adopted band alignment scheme. The scheme is based on the choice of α reproducing the experimental band gap of each interface component (Refs. 5 and 31).

approximation for the exchange-correlation energy proposed by Perdew, Burke, and Ernzerhof (PBE).[28] For the electronic structure, we used the class of hybrid density functionals which are based on the semilocal PBE approximation and are obtained by replacing a fraction α of PBE exchange with Hartree–Fock exchange.[29] For each material, we used the fraction α that reproduced the experimental band gap.

We calculated the band offsets by aligning the band extrema of the bulk interface components through a local reference level at the interface.[30] This procedure relies on the weak dependence of the offset of the local electrostatic potential across the interface on α.[5,31] Hence, the band structures of the individual bulk components are obtained through the use of optimal α's, while the choice of α in the interface calculation is not critical. The band alignment procedure is schematically illustrated in Fig. 1 and has been found to yield band offsets in excellent agreement with experimental values for a series of interface systems.[5,31]

As far as the defect levels are concerned, a recent investigation has shown that they are positioned on an energy scale that is practically unaffected by band-gap renormalization.[32] Hence, hybrid functionals with optimized α modify the position of the band edges but do not significantly affect the relative location of the defect levels in wide band-gap oxides. The application of this scheme to well-characterized defects yields excellent agreement with the experiment.[32,33]

The results presented here were obtained with a plane-wave pseudopotential approach. For the computational settings, we refer to Refs. 5, 20, and 34. We used the QUANTUM-ESPRESSO (Ref. 35) and CPMD (Ref. 36) packages.

III. STRUCTURAL MODELS

To describe the structural environment in the $Si-SiO_2-HfO_2$ stack, we considered both the bulk and the interface models (Fig. 2). To represent the various stack components, we used bulk models of amorphous SiO_2 (Refs. 37 and 38) and amorphous $(HfO_2)_x(SiO_2)_{1-x}$.[34,39,40] The bulk oxide was modeled by monoclinic HfO_2 (m-HfO_2).[41] We generated a model interface between crystalline silicon and amorphous HfO_2 including the SiO_2 interlayer through *ab initio* molecular dynamics.[5] The structural properties of these models will be discussed in the following.

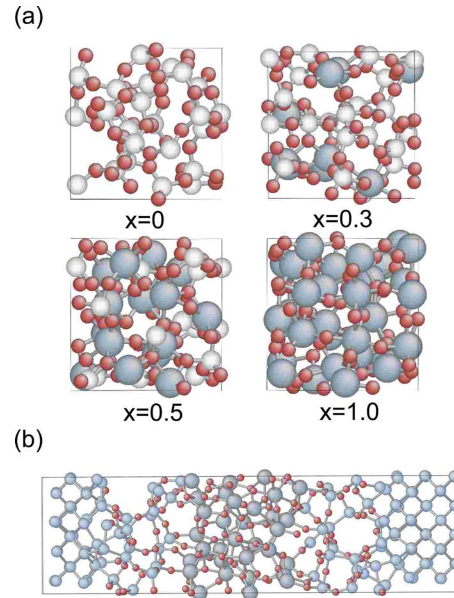

FIG. 2. (Color online) (a) Bulk models of amorphous $(HfO_2)_x(SiO_2)_{1-x}$ (Refs. 34 and 37–40) and (b) interface model of the $Si-SiO_2-HfO_2$ stack (Ref. 5).

A. Bulk models

We generated models for $(HfO_2)_x(SiO_2)_{1-x}$ with $x=0$, 0.3, 0.5, and 1.[34,37–40] The models were generated through constant volume simulations carried out with densities corresponding to zirconium silicates. We used experimental data up to $x=0.5$ and an extrapolation of the linear experimental trend for amorphous HfO_2.[42] Hence, the adopted densities were 2.2, 4.2, 5.8, and 9.1 g/cm^3 for $x=0$, 0.3, 0.5, and 1, respectively. The initial atomic configurations of our simulations were obtained from preliminary classical molecular dynamics runs. The final structures are the result of thermal quenches from the melt at the *ab initio* level of theory.

The generated structures are displayed in Fig. 2(a). In our models, only Hf–O and Si–O bonds occurred. We have characterized the structural evolution from SiO_2 to HfO_2 through the average atomic coordination numbers calculated by integrating the pair correlation functions until their first minima. In amorphous SiO_2, silicon and oxygen were found to be fourfold and twofold coordinated, respectively. Silicon remains fourfold coordinated in all our silicate models ($x=0.3,0.5$). The average Si–O bond lengths increase from 1.64 Å at $x=0$ to 1.66 Å at $x=0.5$, showing a weak dependence on Hf content. For the hafnium coordination, we obtained 5.1, 5.9, and 6.2 for $x=0.3$, 0.5, and 1, respectively. The increase in coordination is accompanied by a small elongation of the average Hf–O bond length: 2.10 Å at $x=0.3$, 2.13 Å at $x=0.5$, and 2.14 Å at $x=1$. The average coordination of the oxygen atoms increases steadily with Hf content, giving coordination numbers of 2.0, 2.2, 2.5, and 3.0 for $x=0$, 0.3, 0.5, and 1, respectively. We note that with increasing Hf content, the hafnium and oxygen coordinations approach those of monoclinic HfO_2, which corresponds to the most

Downloaded 31 Mar 2009 to 128.178.157.61. Redistribution subject to AIP license or copyright; see http://jap.aip.org/jap/copyright.jsp

stable crystalline phase. However, the hafnium and oxygen coordinations in our model of amorphous HfO_2 still remain below the average crystalline values of 7 and 3.5, respectively.

B. Interface model

At the $Si-HfO_2$ interface, the hafnium oxide is amorphous when deposited at low temperatures but transforms to a polycrystalline form upon the thermal annealing required for dopant activation.[43] The transition is characterized by the formation of an amorphous interlayer composed of SiO_2.[43] These experimental aspects have guided the generation of an atomistic interface model.

We generated a model interface between crystalline silicon and amorphous HfO_2 including the amorphous SiO_2 interlayer through *ab initio* molecular dynamics.[5] To avoid the description of outer surfaces, we adopted a superlattice geometry. The attachment of the SiO_2 to the Si(100) substrate was based on previous models of the $Si-SiO_2$ interface, which account for photoemission and ion-scattering experiments.[6,7] We kept 7 Å of SiO_2 on either side of a 10 ML thick Si(100) substrate. The region between the SiO_2 terminations was filled with a HfO_2 layer of ~1.2 nm in accordance with electron counting rules[3] and the experimental density[44] of $\sim 9\ g/cm^3$. The model consisted of 282 atoms. The final structure was generated by evolving the HfO_2 structure at a temperature of 3000 K, while initially keeping the boundary SiO_2 layers frozen. At this temperature, diffusive motion was observed in the HfO_2 layer on the time scale of our simulation (8 ps). After the high-temperature treatment, we applied a thermal quench to $T=0$ K which allowed the full structural model to relax.

The final model structure is shown in Fig. 2(b). The mass density across the HfO_2 layer remained close to the targeted value of $9\ g/cm^3$ and the electronic density of states revealed no localized defect states in the band gap, thereby ensuring a defect free amorphous HfO_2 thin film. The average atomic oxygen concentration is fairly constant at around 2/3 throughout the oxide stack, while the silicon and hafnium concentrations interchange at the SiO_2-HfO_2 interface. As this interface is crossed the oxygen coordination increases from 2 in the SiO_2 to 3 in the HfO_2. At the SiO_2-HfO_2 interface, the oxygen atoms primarily occur in twofold-coordinated local arrangements with hafnium and silicon atoms in their first-neighbor shell. However, other arrangements are also found such as threefold coordinated oxygen atoms either with 2 hafnium and 1 silicon or with 1 hafnium and 2 silicon. The average Hf–O bond length in the model interface is 2.1 Å in good agreement with typical values for amorphous HfO_2. The average hafnium coordination by oxygen increases from 5.7 in the vicinity of the interface to 6.2 in the middle of the HfO_2 layer. The silicon atoms are always fourfold coordinated in our model, but their coordination by oxygen gradually increases across the $Si-SiO_2$ interface.

IV. BAND ALIGNMENTS

Before calculating band offsets, we determined the optimal α that reproduced the band gap of each interface component. For silicon, we used $\alpha=0.11$ for which we obtained the well-characterized band gap of 1.17 eV. In the case of amorphous SiO_2, an α of 0.34 was required to recover the measured band gap of 8.9 eV. While the experimental band gap of m-HfO_2 is well characterized, the measured band gaps of the hafnium containing oxides $[(HfO_2)_x(SiO_2)_{1-x}]$ show a significant scatter.[34] Density functional calculations reveal that the conduction band minimum in the latter materials is determined by hafnium states while the top of the valence band results from oxygen $2p$ states.[34] Therefore, it is reasonable to take a constant value of α for the hafnium containing oxides used in this study $(x>30\%)$ rather than to apply a linear extrapolation scheme between the optimal α for SiO_2 and m-HfO_2. For m-HfO_2, the experimental band gap of 5.8 eV (Ref. 45) was recovered with $\alpha=0.15$. Using this α for crystalline $HfSiO_4$ (hafnon) yielded a band gap of 7.0 eV in reasonably good agreement with the experimental estimate of 6.5–7.0 eV.[46] For amorphous HfO_2 and $HfSiO_4$, we obtained 5.4 and 5.6 eV, in similar good agreement with the experimental data.[47,48]

For the calculation of band offsets, we used local reference levels determined in the interface model to align the band extrema of the various stack components.[30] The procedure is schematically illustrated in Fig. 1. For silicon, the band structure was aligned through the electrostatic potential, while the deep oxygen $2s$ and hafnium $5s$ levels were used for the SiO_2 and hafnium containing components, respectively. The resulting band alignment is schematically illustrated in Fig. 3. In particular, we obtained a 4.4 eV valence band offset between silicon and amorphous SiO_2 in accord with the measured value.[49,50] For the interface between silicon and monoclinic HfO_2, we obtained a valence band offset of 2.9 eV, very close to the measured value of 3.0 eV.[51,52] This level of agreement provides confidence for the quantitative determination of defect levels with respect to the silicon band edges.

V. OXIDE DEFECTS

The generated models were used to study two common oxide defects: the oxygen vacancy and the hydrogen interstitial. The oxygen vacancy has been the object of extensive studies in literature[41,53,54] because it is suspected to be at the origin of the Fermi-level pinning in p-type polysilicon gate stacks.[55,56] The hydrogen interstitial is ubiquitous at such interfaces. While it is known to play a beneficial role in passivating dangling bonds at the $Si-SiO_2$ interface, this impurity may be at the origin of the negative bias temperature instability[57] and the positive charging of the gate oxide.[57,58] To develop a deeper understanding of the role of these defects, we address here their stable charge states and their locations across the dielectric stack.

A. Oxygen vacancy

We examined the relationship between the oxygen vacancy and the Fermi-level pinning.[5] The oxygen vacancy oc-

Downloaded 31 Mar 2009 to 128.178.157.61. Redistribution subject to AIP license or copyright; see http://jap.aip.org/jap/copyright.jsp

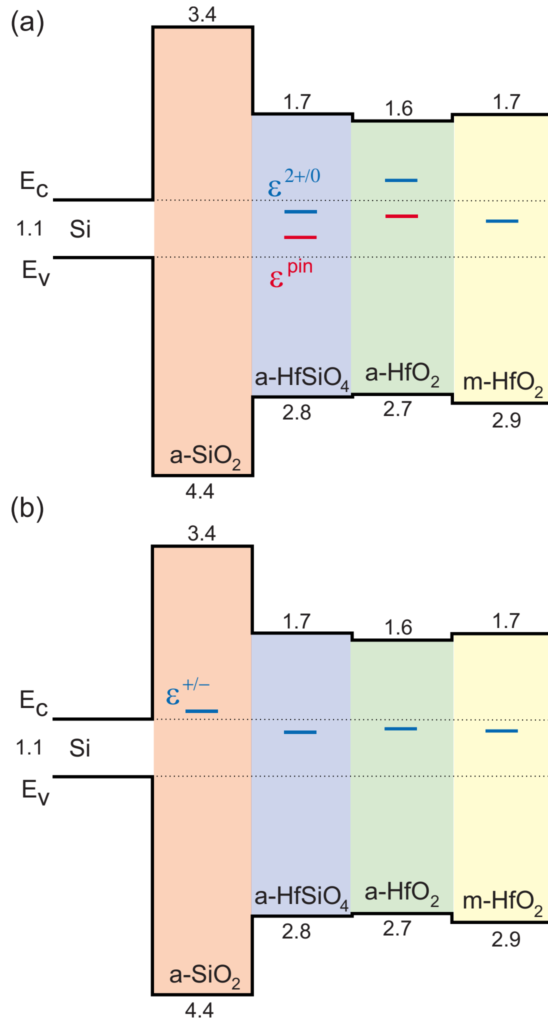

FIG. 3. (Color online) Band alignments in the $Si-SiO_2-HfO_2$ stack composed of Si, amorphous SiO_2, amorphous $HfSiO_4$, amorphous HfO_2, and monoclinic HfO_2. Defect levels associated to (a) the oxygen vacancy and (b) the hydrogen interstitial are indicated. The pinning levels (ϵ_{pin}) associated with the oxygen vacancies are also shown.

curs in several charge states, but the neutral and the doubly positive charge states are the most relevant for Fermi levels falling close to the silicon band edges. Formation energies of these charge states were calculated in each of the hafnium containing components of the gate stack. For both charge states, the calculated formation energy is lower in the amorphous components than in monoclinic HfO_2. The charge transition levels $\epsilon^{2+/0}$ for each component are given in the band diagram of Fig. 3(a). For *p*-type gates, the most stable oxygen vacancy is found for the doubly positive charge state in the amorphous HfO_2 layer. In consideration of the low activation energies for vacancy diffusion across monoclinic HfO_2 (0.7 eV),[59] this result indicates that oxygen vacancies accumulate in this layer, consistent with the experimental observations locating charged defects in the vicinity of the polysilicon gate.[60]

According to the current understanding of Fermi-level pinning in these gate stacks, the oxygen vacancy formation is accompanied by a silicon oxidation reaction.[55,56] The vacancy generation proceeds as long as this reaction is exothermic ($\Delta G<0$),[55,56] thereby fixing the pinning level through the condition $\Delta G=0$. Our results indicate that oxygen vacancies in monoclinic HfO_2 do not lead to Fermi-level pinning. At variance, the amorphous components show pinning levels within the silicon band gap, which account for the position of measured levels.[55,56] Hence, our results for both the energetics and the Fermi-level pinning indicate that oxygen vacancies locate in the noncrystalline transition regions of the gate stack.

B. Hydrogen interstitial

We studied the energetics of various structural configurations and charge states of hydrogen in the $Si-SiO_2-HfO_2$ stack.[20] Hydrogen is found to be amphoteric with a $\epsilon^{+/-}$ charge transition level lying close to the Si conduction band minimum for all stack components [cf. Fig. 3(b)]. In SiO_2, the charge transition level is located just above the silicon conduction band minimum, whereas it is located in the upper part of the silicon band gap for the hafnium-containing stack components. In the positive charge state, the hydrogen interstitial is generally most stable when attached to an oxygen atom which forms two bonds with the oxide network. The negatively charged state corresponds to the hydrogen attached to either silicon or a hafnium atom, the latter being energetically more favorable.

Our results indicate that the proton is the stable charge state of hydrogen across the $Si-SiO_2-HfO_2$ stack for most Fermi levels in the Si band gap in accord with the previous results obtained at the PBE level of theory.[20] The most stable configurations are found in two distinct regions: at the $Si-SiO_2$ interface and toward the HfO_2 layer. At the $Si-SiO_2$ interface, the proton induces the formation of deep positive charge traps consisting of threefold coordinated oxygen atoms.[12] In the hafnium silicates, the most stable states consist of oxygen atoms that are twofold coordinated by hafnium. For instance, the energy of $Hf-OH^+-Hf$ configurations is lower by as much as 1.3 eV with respect to the energy of mobile protons in SiO_2.[20] Furthermore, it is noteworthy that higher proton energies are obtained for oxygen atoms with higher coordinations, which predominate in bulk HfO_2. Hence, we infer that protons in $Si-SiO_2-HfO_2$ stacks are trapped either at the $Si-SiO_2$ interface or at the edge of the HfO_2 layer. These results are consistent with the experiment.[58]

VI. CONCLUSION

It is anticipated that as new materials solutions are screened in the microelectronic technology, the need for a theoretical tool for defect identification will prove ineluctable. In this work, we demonstrated a comprehensive theoretical scheme for determining the band alignment and defect energy levels at semiconductor-oxide interfaces. The scheme is based on the use of hybrid density functionals for the electronic structure and of realistic atomistic models of the interface and its bulk components.

We here applied the scheme to two oxide defects in the technologically important $Si-SiO_2-HfO_2$ stack: the oxygen vacancy and the hydrogen interstitial. It is shown that the scheme reliably reproduces the experimental band alignment

Downloaded 31 Mar 2009 to 128.178.157.61. Redistribution subject to AIP license or copyright; see http://jap.aip.org/jap/copyright.jsp

and that it allows one to locate the defect energy levels with respect to the semiconductor and oxide band edges. The stable charge states of the defects and their location within the dielectric stack can thus be studied as the Fermi level sweeps through the silicon band gap. In particular, our scheme identifies the oxygen vacancy located in the amorphous transition region as a potential candidate for causing Fermi-level pinning in p-type gates.

ACKNOWLEDGMENTS

Financial support from the Swiss National Science Foundation (Grant Nos. 200020-119733 and 200020-111747) is acknowledged. Most of the calculations were performed on the BlueGene of EPFL. We also used the facilities at DIT-EPFL, CSEA-EPFL, and CSCS.

[1] J. Robertson, Eur. Phys. J.: Appl. Phys. **28**, 265 (2004).
[2] A. Pasquarello and A. M. Stoneham, J. Phys.: Condens. Matter **17**, V1 (2005).
[3] P. W. Peacock and J. Robertson, Phys. Rev. Lett. **92**, 057601 (2004).
[4] O. Sharia, A. A. Demkov, G. Bersuker, and B. H. Lee, Phys. Rev. B **75**, 035306 (2007).
[5] P. Broqvist, A. Alkauskas, and A. Pasquarello, Appl. Phys. Lett. **92**, 132911 (2008).
[6] A. Bongiorno, A. Pasquarello, M. S. Hybertsen, and L. C. Feldman, Phys. Rev. Lett. **90**, 186101 (2003).
[7] A. Bongiorno and A. Pasquarello, Appl. Phys. Lett. **83**, 1417 (2003).
[8] F. Giustino and A. Pasquarello, Phys. Rev. Lett. **95**, 187402 (2005).
[9] F. Devynck, F. Giustino, P. Broqvist, and A. Pasquarello, Phys. Rev. B **76**, 075351 (2007).
[10] F. Giustino, A. Bongiorno, and A. Pasquarello, Appl. Phys. Lett. **86**, 192901 (2005).
[11] F. Giustino and A. Pasquarello, Surf. Sci. **586**, 183 (2005).
[12] J. Godet, F. Giustino, and A. Pasquarello, Phys. Rev. Lett. **99**, 126102 (2007).
[13] A. Bongiorno and A. Pasquarello, Phys. Rev. Lett. **88**, 125901 (2002).
[14] A. Bongiorno and A. Pasquarello, Phys. Rev. B **70**, 195312 (2004).
[15] G. A. Baraff, J. A. Appelbaum, and D. R. Hamann, Phys. Rev. Lett. **38**, 237 (1977).
[16] W. E. Pickett, S. G. Louie, and M. L. Cohen, Phys. Rev. B **17**, 815 (1978).
[17] C. G. Van de Walle and R. L. Martin, Phys. Rev. B **35**, 8154 (1987).
[18] S.-H. Wei and A. Zunger, Appl. Phys. Lett. **72**, 2011 (1998).
[19] N. Peressi, N. Binggeli, and A. Baldereschi, J. Phys. D **31**, 1273 (1998).
[20] J. Godet, P. Broqvist, and A. Pasquarello, Appl. Phys. Lett. **91**, 262901 (2007).
[21] S. B. Zhang, D. Tománek, S. G. Louie, M. L. Cohen, and M. S. Hybertsen, Solid State Commun. **66**, 585 (1988).
[22] R. Shaltaf, G.-M. Rignanese, X. Gonze, F. Giustino, and A. Pasquarello, Phys. Rev. Lett. **100**, 186401 (2008).
[23] S. Ismail-Beigi and S. G. Louie, Phys. Rev. Lett. **95**, 156401 (2005).
[24] M. Hedström, A. Schindlmayr, G. Schwarz, and M. Scheffler, Phys. Rev. Lett. **97**, 226401 (2006).
[25] L. A. Curtiss, P. C. Redfern, K. Raghavachari, and J. A. Pople, J. Chem. Phys. **109**, 42 (1998).
[26] J. Muscat, A. Wander, and N. M. Harrison, Chem. Phys. Lett. **342**, 397 (2001).
[27] J. Paier, M. Marsman, K. Hummer, G. Kresse, I. C. Gerber, and J. G. Ángyán, J. Chem. Phys. **124**, 154709 (2006); **125**, 249901 (2006).
[28] J. P. Perdew, K. Burke, and M. Ernzerhof, Phys. Rev. Lett. **77**, 3865 (1996).
[29] J. P. Perdew, M. Ernzerhof, and K. Burke, J. Chem. Phys. **105**, 9982 (1996).
[30] C. G. Van de Walle and R. M. Martin, Phys. Rev. B **34**, 5621 (1986).
[31] A. Alkauskas, P. Broqvist, F. Devynck, and A. Pasquarello, Phys. Rev. Lett. **101**, 106802 (2008).
[32] A. Alkauskas, P. Broqvist, and A. Pasquarello, Phys. Rev. Lett. **101**, 046405 (2008).
[33] P. Broqvist, A. Alkauskas, and A. Pasquarello, Phys. Rev. B **78**, 075203 (2008).
[34] P. Broqvist and A. Pasquarello, Appl. Phys. Lett. **90**, 082907 (2007).
[35] A. Pasquarello, K. Laasonen, R. Car, C. Lee, and D. Vanderbilt, Phys. Rev. Lett. **69**, 1982 (1992); K. Laasonen, A. Pasquarello, R. Car, C. Lee, and D. Vanderbilt, Phys. Rev. B **47**, 10142 (1993); we used the implementation provided by http://www.quantum-espresso.org/.
[36] CPMD, Copyright IBM Corp. 1990–2006, Copyright MPI für Festkörperforschung Stuttgart, 1997.
[37] J. Sarnthein, A. Pasquarello, and R. Car, Phys. Rev. Lett. **74**, 4682 (1995).
[38] J. Sarnthein, A. Pasquarello, and R. Car, Phys. Rev. B **52**, 12690 (1995).
[39] P. Broqvist and A. Pasquarello, Microelectron. Eng. **84**, 2416 (2007).
[40] P. Broqvist and A. Pasquarello, Microelectron. Eng. **84**, 2022 (2007).
[41] P. Broqvist and A. Pasquarello, Appl. Phys. Lett. **89**, 262904 (2006).
[42] M. Nogami, J. Non-Cryst. Solids **69**, 415 (1985).
[43] G. D. Wilk and D. A. Muller, Appl. Phys. Lett. **83**, 3984 (2003).
[44] M. Modreanu, J. Sanho-Parramon, D. O'Connell, J. Justice, O. Durand, and B. Servet, Mater. Sci. Eng., B **118**, 127 (2005).
[45] S.-G. Lim, S. Kriventsov, T. N. Jackson, J. H. Haeni, D. G. Schlom, and A. M. Balbasov, J. Appl. Phys. **91**, 4500 (2002).
[46] P. W. Peacock and J. Robertson, J. Appl. Phys. **92**, 4712 (2002).
[47] H. Takeuchi, D. Ha, and T.-J. King, J. Vac. Sci. Technol. A **22**, 1337 (2004).
[48] H. Jin, S. K. Oh, H. J. Kang, and M.-H. Cho, Appl. Phys. Lett. **89**, 122901 (2006).
[49] F. J. Himpsel, F. R. McFeely, A. Teleb-Ibrahimi, J. A. Yarmoff, and G. Hollinger, Phys. Rev. B **38**, 6084 (1988).
[50] J. W. Keister, J. E. Rowe, J. J. Kolodziej, H. Niimi, T. E. Madey, and G. Lucovsky, J. Vac. Sci. Technol. B **17**, 1831 (1999).
[51] M. Oshima, S. Toyoda, T. Okumura, J. Okabayashi, H. Kumigashira, K. Ono, M. Niwa, K. Usuda, and N. Hirashita, Appl. Phys. Lett. **83**, 2172 (2003).
[52] O. Renault, N. T. Barrett, D. Samour, and S. Quiais-Marthon, Surf. Sci. **566–568**, 526 (2004).
[53] K. Xiong, J. Robertson, M. C. Gibson, and S. J. Clark, Appl. Phys. Lett. **87**, 183505 (2005).
[54] J. L. Gavartin, D. Munoz Ramo, A. L. Schluger, G. Bersuker, and B. H. Lee, Appl. Phys. Lett. **89**, 082908 (2006).
[55] K. Shiraishi, K. Yamada, K. Torii, Y. Akasaka, K. Nakajima, M. Konno, T. Chikyo, H. Kitajima, and T. Arikado, Jpn. J. Appl. Phys., Part 2 **43**, L1413 (2004).
[56] K. Shiraishi, H. Takeuchi, Y. Akasaka, H. Watanabe, N. Umezawa, T. Chikyow, Y. Nara, T.-J. King Liu, and K. Yamada, Proceedings of the IEEE International Conference on Simulation of Semiconductor Processes and Devices, 2006 (unpublished), p. 306.
[57] M. Houssa, S. D. Gendt, J. L. Autran, and G. Groeseneken, Appl. Phys. Lett. **85**, 2101 (2004).
[58] V. V. Afanas'ev and A. Stesmans, J. Appl. Phys. **95**, 2518 (2004).
[59] N. Capron, P. Broqvist, and A. Pasquarello, Appl. Phys. Lett. **91**, 192905 (2007).
[60] V. V. Afanas'ev and A. Stesmans, J. Appl. Phys. **102**, 081301 (2007).

Downloaded 31 Mar 2009 to 128.178.157.61. Redistribution subject to AIP license or copyright; see http://jap.aip.org/jap/copyright.jsp